

## Charge effects in the structure of an almost-ionic solid: Molecular-dynamics studies

J. Trullàs, A. Giró, and R. Fontanet

*Departament de Física i Enginyeria Nuclear, Universitat Politècnica de Catalunya,  
Mòdul B5, Campus Nord, E-08034 Barcelona, Spain*

M. Silbert

*School of Physics, University of East Anglia, Norwich NR4 7TJ, United Kingdom*

(Received 18 April 1994; revised manuscript received 13 July 1994)

The molecular-dynamics studies reported in this work concern the behavior of a system, with a pair-potential model appropriate for CuI, as a function of its charge  $|Z|$ . These studies are carried out at two temperatures. The lower at  $T=625$  K, corresponds to its  $\gamma$  phase; the higher, at  $T=700$  K, to its  $\alpha$  phase. The structure of the system in the  $\gamma$  phase at  $|Z|=0.6$  is zinc-blende. When the charge is lowered to  $|Z|=0.3$  the system is found in a rocksalt structure. At  $|Z|=0.2$  the structure is still rocksalt, but the cations now diffuse through hopping. At  $|Z|=0$  it is found in the molten state. In the  $\alpha$  phase, at  $|Z|=0.6$ , the system is superionic with the anions sitting on a fcc sublattice while the cations exhibit a liquidlike structure. For  $|Z|=0.2$ , the system is found in a rocksalt structure, and is no longer superionic. When the charge is completely removed the system is again found in the molten state. The lowering of the charge in this model almost-ionic solid appears to exhibit effects akin to those found by increasing its pressure.

### I. INTRODUCTION

The noble-metal halides form a very interesting group of compounds which Tosi<sup>1</sup> has named "almost ionic." The low-temperature solid phase of the copper halides and of AgI exhibit a zinc-blende structure and are at the extreme ionic end of a sequence of tetrahedrally coordinated compounds of the  $A^N B^{8-N}$  type.<sup>2</sup> The zinc-blende structure becomes unstable when these compounds are subjected to hydrostatic pressure, and as a result, a solid phase transformation takes place to a rocksalt structure, which, in the case of the copper halides and AgI, is normally achieved through passage to intermediate structures.<sup>3</sup> Under ambient-pressure conditions, as the temperature is increased, these systems experience a phase transition from a normal to a fast ionic phase, the  $\alpha$  phase; namely, the anion sublattice remains localized, while the cation sublattice is diffusive.<sup>4</sup> Actually, CuCl has no  $\alpha$  phase, but its ionic conductivity is comparable to that of the other cuprous halides in both its low- and high-temperature phases. Moreover, there is experimental evidence, at least for AgI,<sup>5</sup> that on increasing the temperature, the high-pressure rocksalt structure undergoes a continuous transition to an  $\alpha$  phase, similar to that reported for several materials with fluorite structure. The mechanism which induces this continuous phase transition is also likely to be responsible for the strong premelting phenomena observed in AgCl and AgBr.<sup>6,7</sup>

Ionic melts also experience continuous structural phase transitions. Shock-wave experiments<sup>8</sup> and theoretical calculations<sup>9</sup> along the melting line show that the alkali-halide melts undergo a gradual pressure-induced structural change from a rocksalt structure to one that has a rare-gas-like close arrangement. Following computer-simulation work on the charge-ordering effects in the noble-metal halides,<sup>10</sup> it has been suggested that

these melts also experience a continuous pressure-induced structural transition along the melting line.<sup>11</sup> This suggestion is based on the observation that the effects of reducing the effective charge of the ions in molten salts appear to be similar to those of increasing the pressure of the system. As the charge is reduced, the potential of the interaction between the ions changes. Specifically, the depth of the attractive Coulomb interaction between unlike ions is shallower, thus requiring a higher pressure to keep the system together at constant temperature and density.

In this work we study the effects of reducing the change in a model solid almost-ionic compound using molecular-dynamics simulations. The potentials used here are the same as those proposed by Vashishta and Rahman<sup>12,13</sup> for CuI, and there is a large size difference between the (smaller) cations and anions.

A study of structural transitions is not possible within the framework of the standard molecular-dynamics (MD) technique used in this work. Here we are solely concerned with the structure of the system under study found in a given thermodynamic state as a function of charge. This information is provided by the pair distribution functions of the component species,  $g_{\alpha\beta}(r)$ .

Moreover, we are interested in learning about the diffusion mechanisms in the different thermodynamic states through the mean-square displacements  $\langle r_\alpha^2(t) \rangle$  and the normalized velocity autocorrelation functions  $C_\alpha(t)$  of the component species. The subscripts  $\alpha, \beta$  denote, in all cases, the species for which these properties are evaluated ( $\alpha, \beta \equiv +, -$ ).

We note that a detailed comparison with experiment is out of the scope of this paper. For even if the potentials of interaction used in this work were moderately realistic for CuI, the removal of charge from the system is a construct which cannot be realized experimentally.

The layout of the paper is as follows. A brief description of the potentials, the actual method used in the simulations, and a definition of the properties we study are given in the next section. The results of the simulations are presented in Sec. III. Finally, a brief summary and discussion of the results are given in Sec. IV.

## II. DEFINITIONS

The effective pair potentials are of the form<sup>12,13</sup>

$$\begin{aligned}\Phi_{++}(r) &= \frac{Z^2 e^2}{r} + \Phi_{++}^0(r), \\ \Phi_{--}(r) &= \frac{Z^2 e^2}{r} - \frac{\alpha_- Z^2 e^2}{r^4} - \frac{C_{--}}{r^6} + \Phi_{--}^0(r), \\ \Phi_{+-}(r) &= -\frac{Z^2 e^2}{r} - \frac{1}{2} \frac{\alpha_- Z e^2}{r^4} + \Phi_{+-}^0(r),\end{aligned}\quad (1)$$

where

$$\Phi_{\alpha\beta}^0(r) = \frac{H_{\alpha\beta}}{r^7} \quad (\alpha, \beta \equiv +, -), \quad (2)$$

for which we use the parameters listed in Table I.<sup>13</sup>

For the MD simulations we take a set of  $N = 216$  particles ( $N/2$  cations,  $N/2$  anions) placed in a cubic box with periodic boundary conditions. Both the number of particles and boundary conditions used are appropriate for the type of calculations carried out.<sup>14</sup> We have used Beeman's algorithm<sup>15</sup> with a time step  $\Delta t = 0.6 \times 10^{-2}$  ps and the Ewald method to account for the long-range Coulomb interaction.<sup>16</sup> Once the system reaches equilibrium, the correlation functions were calculated by taking a time average.

We have calculated the pair distribution functions  $g_{\alpha\beta}(r)$ , the mean-square displacements

$$\langle r_\alpha^2(t) \rangle = \frac{1}{N_\alpha} \sum_{\alpha_i=1}^{N_\alpha} \langle |\mathbf{r}_{\alpha_i}(t) - \mathbf{r}_{\alpha_i}(0)|^2 \rangle, \quad (3)$$

and the normalized velocity autocorrelation functions

$$C_\alpha(t) = \frac{\Psi_\alpha(t)}{\Psi_\alpha(0)}, \quad (4)$$

where

$$\Psi_\alpha(t) = \frac{1}{N_\alpha} \sum_{\alpha_i=1}^{N_\alpha} \langle \mathbf{v}_{\alpha_i}(t) \cdot \mathbf{v}_{\alpha_i}(0) \rangle. \quad (5)$$

We have also evaluated the self-diffusion coefficients  $D_\alpha$ . These are obtained by using either the Einstein relation

$$D_\alpha = \lim_{t \rightarrow \infty} \frac{\langle r_\alpha^2(t) \rangle}{6t} \quad (6)$$

or the Kubo formula

$$D_\alpha = \frac{1}{3} \int_0^\infty \Psi_\alpha(t) dt. \quad (7)$$

In our simulations we evaluate both and the results quoted are normally an average of the two values.

TABLE I. Values of the parameters given by Eqs. (1) and (2). Units of length are given in angstroms (Å) and energy in 14.39 eV.

$H_{++}$	$H_{--}$	$H_{+-}$	$\alpha_-$	$C_{--}$
0.011 96	339.578	12.982	6.52	6.93

## III. RESULTS

We carried out simulations at three different temperatures. The first, at  $T = 625$  K, corresponds to the  $\gamma$  phase of CuI. The other two, at  $T = 700$  and  $834$  K, correspond to its  $\alpha$  phase. In all cases simulations were carried out for values of the charge  $|Z| = 0.6, 0.2,$  and  $0.0$ . The first of these values is the one which accounts correctly for the  $\gamma$ -to- $\alpha$  transition in CuI at normal pressures.<sup>17</sup> We also carried out a further calculation at  $T = 625$  K with  $|Z| = 0.3$ . In all the simulations we kept the density constant at  $\rho = 0.0344$  ions/Å<sup>3</sup>.

### A. Simulations of the $\gamma$ phase

The system was placed, with charge  $|Z| = 0.6$ , in a zinc-blende configuration. The kinetic energy was increased until the system reached a temperature  $T = 625$  K. Equilibration was attained after about 5000 time steps.  $g_{\alpha\beta}(r)$ ,  $\langle r_\alpha^2(t) \rangle$ , and  $C_\alpha(t)$  were estimated by taking time averages over, approximately, 20 000 time steps. The number of time steps used was found to be adequate for the properties in this work. Values for the self-diffusion constants  $D_\alpha$ , however, have an error bar of 5–10 %. The same procedure was used in all the simulations.

The results for  $g_{\alpha\beta}(r)$ ,  $\langle r_\alpha^2(t) \rangle$ , and  $C_\alpha(t)$  are shown in Figs. 1(a), 3(a), and 4(a), respectively. The coordination numbers of the first coordination shell in  $g_{\alpha\beta}(r)$  were evaluated from the standard relation

$$N_{\alpha\beta} = 4\pi\rho \int_0^R r^2 g_{\alpha\beta}(r) dr, \quad (8)$$

where  $R$  denotes the position of the first minima in the  $g_{\alpha\beta}(r)$ . The values of  $N_{\alpha\beta}$  are given in Table II and correspond to those expected for a zinc-blende structure. Moreover, the positions of the successive peaks of the  $g_{\alpha\beta}(r)$  are in excellent agreement with those expected for this particular crystal structure. The results for  $\langle r_\alpha^2(t) \rangle$  and  $C_\alpha(t)$  are consistent with the anions and cations oscillating around their equilibrium positions.

We now turn to the case  $|Z| = 0.3$ . We used as the initial configuration one of the stable configurations of the previous case and then reduced the charge to 0.3.

After equilibration was attained the system exhibited a rocksalt structure, as shown by the  $g_{\alpha\beta}(r)$  in Fig. 1(b). Both  $g_{++}(r)$  and  $g_{--}(r)$  are similar to those found for  $|Z| = 0.6$ , but  $g_{+-}(r)$  is different. We compare, in Fig. 2,  $g_{+-}(r)$  for the two values  $|Z| = 0.6$  and  $0.3$ . The values for the coordination numbers  $N_{\alpha\beta}$  are also shown in Table II. The results for  $\langle r_\alpha^2(t) \rangle$  and  $C_\alpha(t)$ , shown in Figs. 3(b) and 4(b), are again consistent with the anions and cations oscillating around their equilibrium posi-

TABLE II. Coordination numbers and self-diffusion coefficients ( $\gamma$  phase,  $T = 625$  K).

Charge $ Z $	Coordination numbers			Positions of first maxima ( $\text{\AA}$ )			Self-diffusion coefficients ( $10^{-5} \text{ cm}^2 \text{ s}^{-1}$ )	
	$N_{++}$	$N_{--}$	$N_{+-}$	$g_{++}(r)$	$g_{--}(r)$	$g_{+-}(r)$	$D_+$	$D_-$
0.6	12.3	12.0	4.0	4.3	4.3	2.5	0.0	0.0
0.3	12.2	12.0	6.0	4.4	4.3	3.0	0.0	0.0
0.2	12.1	12.0	6.0	4.4	4.3	3.0	0.6	0.0
0.0	38.0	12.1	3.2	1.4	4.1	3.2	2.0	0.2 <sup>a</sup>

<sup>a</sup>In this case the relative error is about 50%.

TABLE III. Coordination numbers and self-diffusion coefficients ( $\alpha$  phase,  $T = 700$  K).

Charge $ Z $	Coordination numbers			Positions of first maxima ( $\text{\AA}$ )			Self-diffusion coefficients ( $10^{-5} \text{ cm}^2 \text{ s}^{-1}$ )	
	$N_{++}$	$N_{--}$	$N_{+-}$	$g_{++}(r)$	$g_{--}(r)$	$g_{+-}(r)$	$D_+$	$D_-$
0.6	12.2	12.0	4.2	4.3	4.3	2.5	4.4	0.0
0.2	12.9	12.0	6.0	4.4	4.3	2.9	1.6	0.0
0.0	41.0	12.5	3.3	1.4	4.1	3.1	2.7	0.2 <sup>a</sup>

<sup>a</sup>In this case the relative error is about 50%.

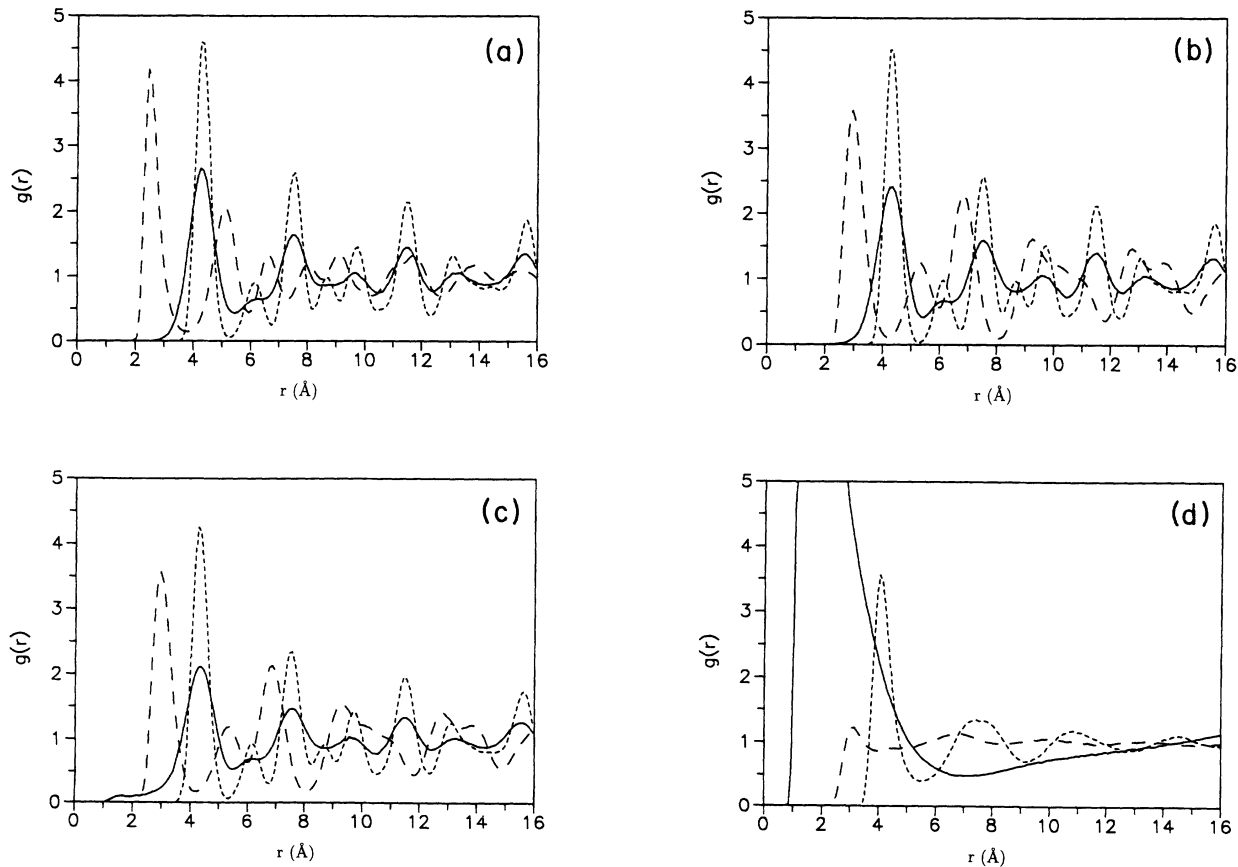


FIG. 1. Pair distribution functions  $g_{\alpha\beta}(r)$  in the  $\gamma$  phase for a system interacting with the potentials given by Eqs. (1) and (2) (see text) at temperature  $T = 625$  K and ionic density  $\rho = 0.0344 \text{ ions/\AA}^3$ , for different values of the charge  $|Z|$ . Solid line,  $g_{++}(r)$ ; dotted line,  $g_{--}(r)$ ; dashed line,  $g_{+-}(r)$ . (a)  $|Z| = 0.6$ , (b)  $|Z| = 0.3$ , (c)  $|Z| = 0.2$ , and (d)  $|Z| = 0$ . In (d) the value of the first peak of  $g_{+-}$  is 13.76.

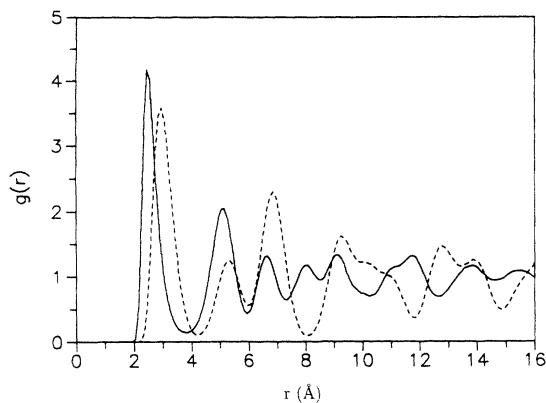


FIG. 2. Pair distribution functions  $g_{+-}(r)$  in the  $\gamma$  phase for the system defined by the caption of Fig. 1. Solid line,  $|Z|=0.6$ ; dashed line,  $|Z|=0.3$ .

tions. However, the backscattering in  $C_+(t)$  means the ions are rattling more than in the  $|Z|=0.6$  case.

At  $|Z|=0.2$  the structure is also rocksalt, but as shown in Fig. 1(c), the peaks of  $g_{\alpha\beta}(r)$  are lower and broader than for  $|Z|=0.3$ . The prepeak at small  $r$  in  $g_{++}(r)$  suggests there is a finite probability of finding more than one

cation in the interstitial cage made by the anions. These interstitial cations are the contributions to the diffusion process, as seen from the results for  $\langle r_+^2(t) \rangle$  [Fig. 3(c)], and which takes place by hopping, as inferred from  $g_{++}(r)$  and  $C_+(t)$  shown in Figs. 1(c) and 4(c).

The mean-square displacements of the cations  $\langle r_+^2(t) \rangle$ , in Fig. 3(b), show a small increase for small  $t$  which may appear surprising. This feature is, in our view, due to the displacements of the cations and also because their velocities [see  $C_+(t)$  in Fig. 4(b)] are strongly correlated at short times. The same feature is also present when the cations diffuse by hopping [see Figs. 3(c) and 4(c)].

At  $|Z|=0.0$  equilibration yields a molten binary mixture similar to that found in our study of charge effects in a superionic melt.<sup>10</sup> The slope of  $\langle r_-^2(t) \rangle$ , shown in Fig. 3(d), is indicative of the liquid state. The pair distribution functions of the neutral system are shown in Fig. 1(d). The average coordination number of the larger atoms is 12. The smaller atoms cluster in the interstitials left by the packing of the larger atoms. In fact, the first peak of the pair distribution function of the smaller atoms samples the average size of this cluster. The mean-square displacement  $\langle r_+^2(t) \rangle$  [Fig. 3(d)] shows two distinctive slopes. The first, for times  $t < 2.0$  ps, reveals

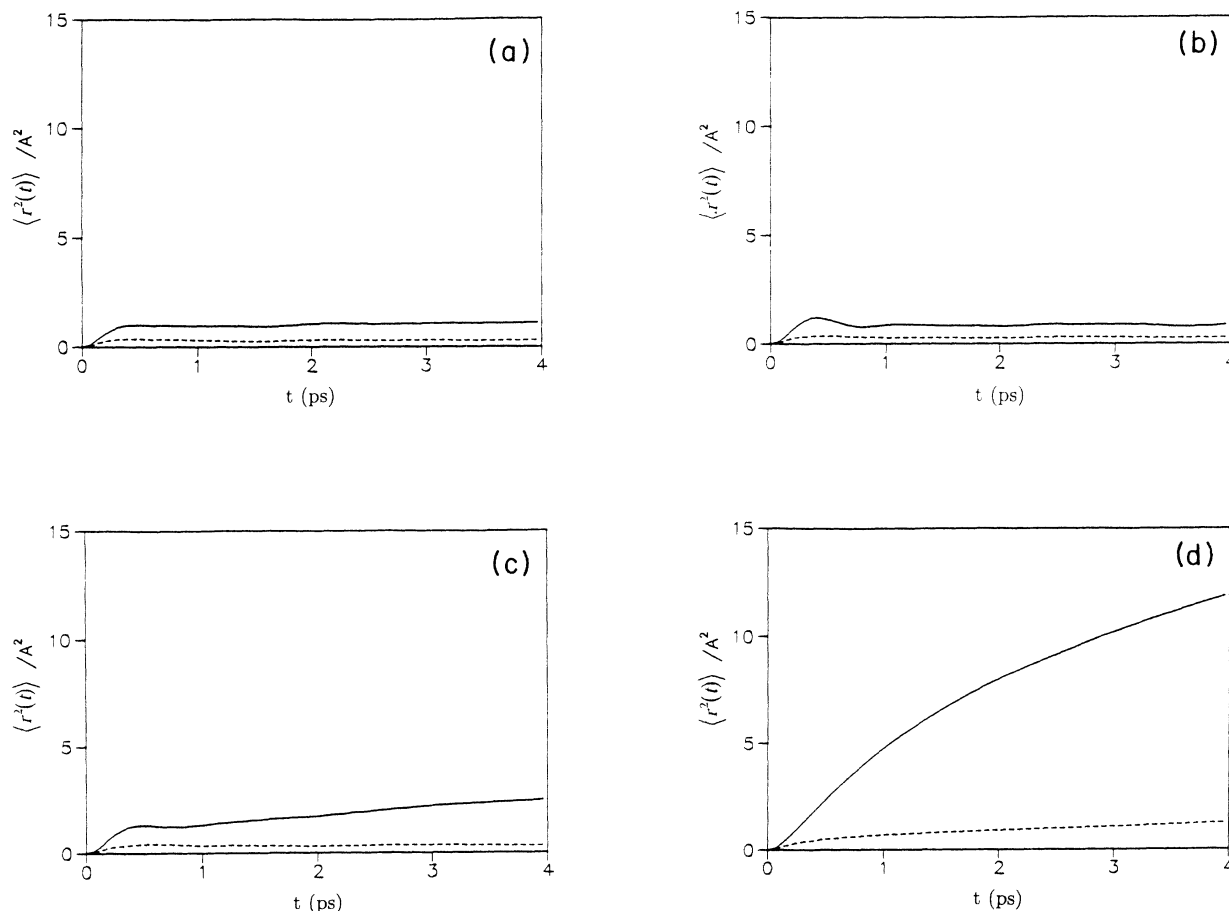


FIG. 3. Mean-square displacements  $\langle r_\alpha^2(t) \rangle$  in the  $\gamma$  phase for the system defined by the caption of Fig. 1. Solid line,  $\langle r_+^2(t) \rangle$ ; dotted line,  $\langle r_-^2(t) \rangle$ . (a)  $|Z|=0.6$ , (b)  $|Z|=0.3$ , (c)  $|Z|=0.2$ , and (d)  $|Z|=0$ .

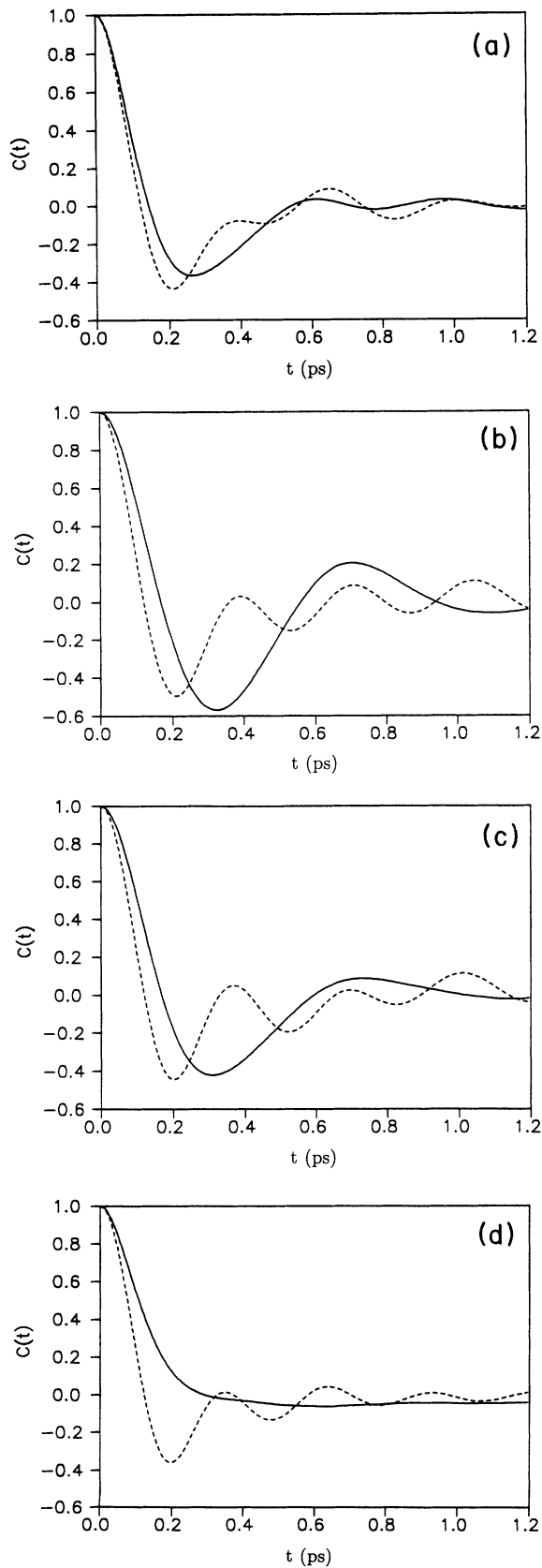


FIG. 4. Normalized velocity autocorrelation functions  $C_\alpha(t)$  in the  $\gamma$  phase for the system defined by the caption of Fig. 1. Solid line,  $C_+(t)$ ; dotted line,  $C_-(t)$ . (a)  $|Z|=0.6$ , (b)  $|Z|=0.3$ , (c)  $|Z|=0.2$ , and (d)  $|Z|=0$ .

the diffusion of the smaller atoms within the cluster; the second shows their diffusive motion after they break through the cage of the larger atoms. The short time diffusive regime is clearly shown in  $C_+(t)$  [Fig. 4(d)]. The value of the diffusion constant  $D_+$  is given in Table II.

### B. MD simulations of the $\alpha$ phase

The MD simulations were carried out at two temperatures  $T=700$  and  $834$  K, which are within the range

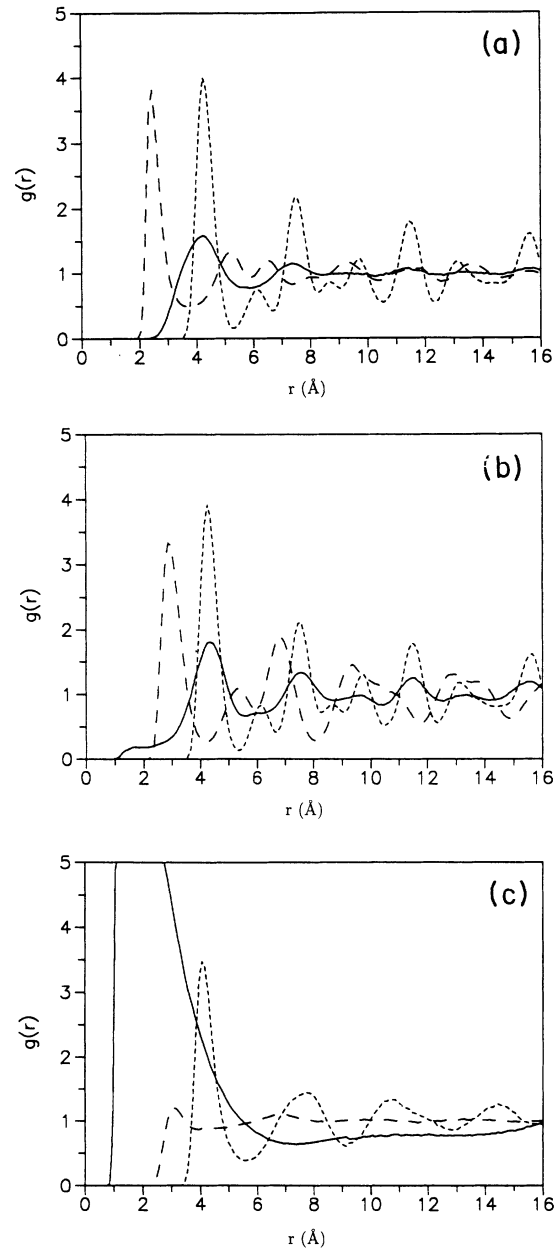


FIG. 5. Pair distribution functions  $g_{\alpha\beta}(r)$  in the  $\alpha$  phase for a system interacting with the potentials given by Eqs. (1) and (2) (see text) at temperature  $T=700$  K and ionic density  $\rho=0.0344$  ions/ $\text{\AA}^3$ , for different values of the charge  $|Z|$ . Solid line,  $g_{++}(r)$ ; dotted line,  $g_{--}(r)$ ; dashed line,  $g_{+-}(r)$ . (a)  $|Z|=0.6$ , (b)  $|Z|=0.2$ , and (c)  $|Z|=0$ . In (c) the value of the first peak of  $g_{+-}$  is 12.95.

TABLE IV. Coordination numbers and self-diffusion coefficients ( $\alpha$  phase,  $T = 834$  K).

Charge $ Z $	Coordination numbers			Positions of first maxima ( $\text{\AA}$ )			Self-diffusion coeffi- cients ( $10^{-5} \text{ cm}^2 \text{ s}^{-1}$ )	
	$N_{++}$	$N_{--}$	$N_{+-}$	$g_{++}(r)$	$g_{--}(r)$	$g_{+-}(r)$	$D_+$	$D_-$
0.6	14.0	12.0	4.5	4.2	4.3	2.5	6.4	0.0
0.2	15.9	12.1	6.1	4.4	4.3	2.9	4.0	0.0
0.0	55.8	11.9	2.6	1.4	4.1	3.1	3.5	0.3 <sup>a</sup>

<sup>a</sup>In this case the relative error is about 50%.

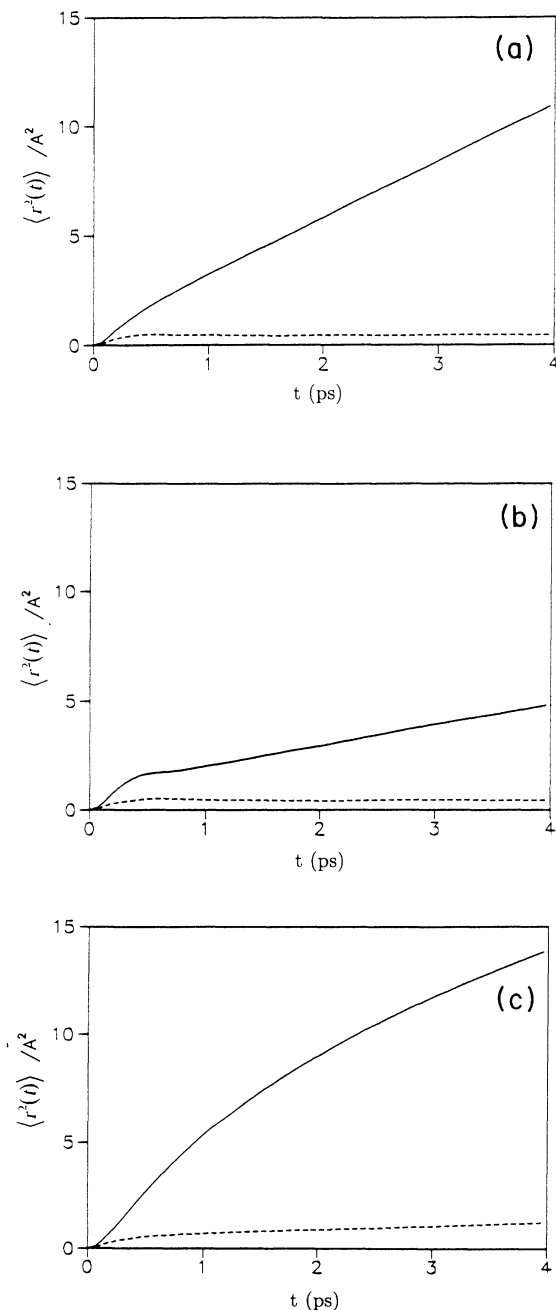


FIG. 6. Mean-square displacements  $\langle r^2(t) \rangle$  in the  $\alpha$  phase for the system defined by the caption of Fig. 5. Solid line,  $\langle r_+^2(t) \rangle$ ; dotted line,  $\langle r_-^2(t) \rangle$ . (a)  $|Z|=0.6$ , (b)  $|Z|=0.2$ , and (c)  $|Z|=0$ .

covered by the  $\alpha$  case of CuI. Since the results at both temperatures are qualitatively similar, only those for the lower  $T$  are presented in full (Table III and Figs. 5–7). In Table IV we include, for completeness, the coordination numbers, positions of the first maxima of the pair distribution functions, and self-diffusion coefficients for  $T = 834$  K.

The simulations were set up as follows. For  $|Z|=0.6$  we chose a stable configuration in the  $\gamma$  phase and then increased the kinetic energy to reach the temperature  $T = 700$  K. For the case  $|Z|=0.2$ , two different procedures were used. The first was to choose a stable configuration at  $T = 700$  K and reduce the charge from  $|Z|=0.6$  to 0.2. In the second we chose a stable configuration at  $T = 625$  K and then increased the kinetic energy to reach  $T = 700$  K. We find the configurations generated by both procedures to be the same within the statistical errors of the simulations. The case  $|Z|=0$  was generated by removing the charge from a stable configuration at  $T = 700$  K and  $|Z|=0.2$ .

The results obtained for  $|Z|=0.6$  are the same as those obtained by Rahman and Vashishta.<sup>17</sup> The anions sit on a fcc sublattice with the same values for the coordination numbers and position of the peaks of  $g_{--}(r)$  as found at  $T = 625$  K (see Table III). Figure 5(a) shows that, for this case, the peaks of  $g_{--}(r)$  are lower and broader than at  $T = 625$  K. The unlike ions have a fourfold coordination. The cations exhibit a typical liquidlike structure, as seen in Fig. 5(a). This picture is supported by the results obtained for  $\langle r_+^2(t) \rangle$ , shown in Fig. 6(a), and  $C_+(t)$ , shown in Fig. 7(a).  $\langle r_-^2(t) \rangle$  is flat, and the backscattering in  $C_-(t)$  reveals oscillations of the anions around their fcc equilibrium positions. On the other hand,  $\langle r_+^2(t) \rangle$  shows that the cations are mobile, with a diffusion constant  $D_+ = 4.4 \times 10^{-5} \text{ m}^2 \text{ s}^{-1}$ . Moreover, the results for  $C_+(t)$  show a distinct diffusive regime. The picture emerging from the simulations at  $T = 834$  K is qualitatively the same, but the cations are now more mobile with a value for  $D_+$  larger by 50% than that given above (see Table IV).

For  $|Z|=0.2$  the stable configuration is one in which the system exhibits a rocksalt structure, similar to that found at  $T = 625$  K with the differences expected for a system at a higher temperature. The prepeak in  $g_{++}(r)$  at  $r \cong 1.5 \text{ \AA}$ , already noted at  $T = 625$  K, is also present at  $T = 700$  K [Fig. 5(b)] and is even more pronounced at  $T = 834$  K. The availability of more cations in interstitial sites favors their mobility, as shown by the slope of  $\langle r_+^2(t) \rangle$  in Fig. 6(b). The diffusion mechanism is by hop-

ping, which is deduced from  $g_{++}(r)$  and the amount of backscattering present in  $C_+(t)$  [Fig. 7(b)]. There are, however, important differences when comparing the stable configurations at  $T=700$  K for  $|Z|=0.6$ , discussed above, and  $|Z|=0.2$ . Since most of the cations in the latter sit on their fcc sublattice, their mobility is lower, as seen by comparing  $\langle r_+^2(t) \rangle$  of Figs. 6(a) and 6(b). This is in marked contrast when the results for these two charges are compared at the lower temperature  $T=625$  K, in Figs. 3(a) and 3(c).

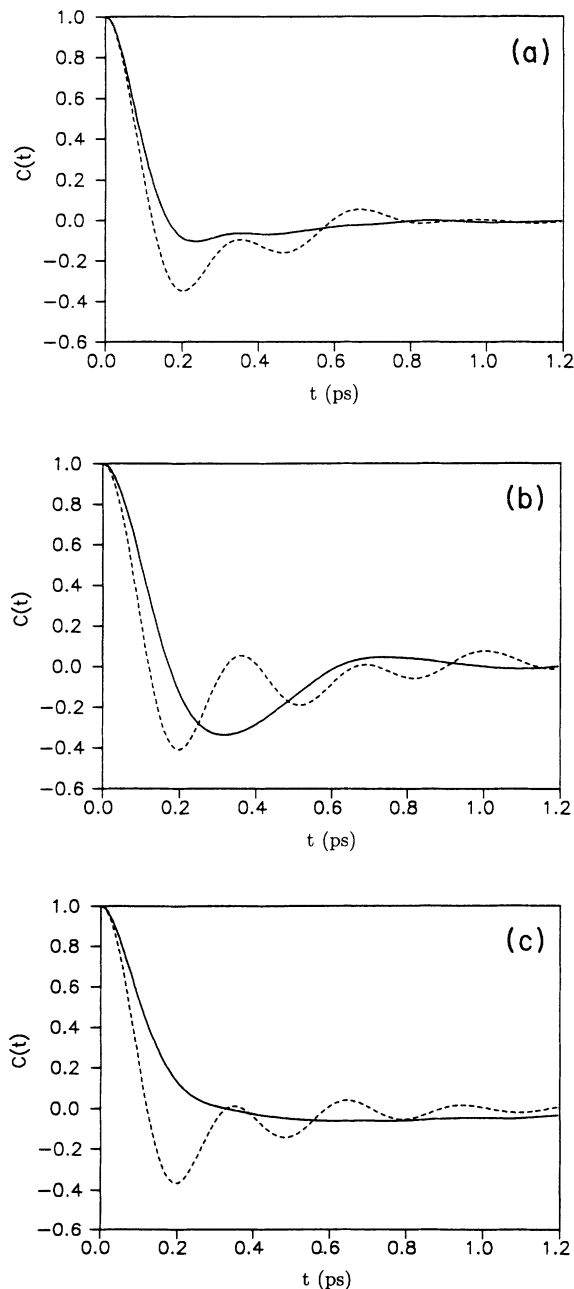


FIG. 7. Normalized velocity autocorrelation functions  $C_\alpha(t)$  in the  $\alpha$  phase for the system defined by the caption of Fig. 5. Solid line,  $C_+(t)$ ; dotted line,  $C_-(t)$ . (a)  $|Z|=0.6$ , (b)  $|Z|=0.2$ , and (c)  $|Z|=0$ .

Finally, at  $|Z|=0$ , the  $g_{\alpha\beta}(r)$ , shown in Fig. 5(c), are similar to those found at  $T=625$  K, but with a small increase in the size of the cluster of the smaller atoms. These are now more mobile both within and outside the cage made up by the larger atoms.

#### IV. DISCUSSION

This work has looked into the properties of model almost-ionic solid compounds as function of charge in their stable configuration using potentials known to be moderately successful in accounting for the  $\gamma \rightarrow \alpha$  transition and the molten structure of CuI.

The different structures may be regarded as a sequence of model binary compounds with decreasing ionicity. Alternatively, they could be regarded as a sequence of structures which a system such as CuI will exhibit when subjected to hydrostatic pressure. Although the approach used here is rather crude, it does provide valuable insights into the ordering which takes place in the different structures, which will be of assistance in attempting more realistic calculations. For instance, as in the experimental results of CuI under pressure,<sup>18</sup> we find that the iodine sublattice remains a nearly ideal fcc lattice. This, in turn, suggests that the class of potentials used here is capable of reproducing the main structural trends of the noble-metal halides under pressure.

Further progress can be made in two fronts. As stated in the Introduction, in the simulation code used in this work both the shape and size of the MD cell remain fixed. This precludes the study of structural transitions. Such a study requires a generalization of the MD technique, originally introduced by Parrinello and Rahman<sup>19</sup> and known as constant-stress MD, which allows the dynamical variables describing both the size and shape of the MD cell to fluctuate so as to maintain constant stress. This code, which we are currently incorporating in our programs, has made it possible to outline the broad features of the phase diagram of AgI.<sup>20</sup> We expect to use this code to study the phase diagram of the remaining noble-metal halides.

The electronic structure of the copper halides under pressure undergoes important changes, particularly in the  $d-p$  interaction between the noble-metal  $3d$  states and the halogen  $p$  states.<sup>18</sup> This, in turn, results in subtle changes in the potentials of the interaction which we are only taking into account in a very crude manner. These changes in the potentials of the interaction may be responsible for the existence of intermediate structures in CuI.<sup>21,22</sup> The description of these intermediate structures may therefore require going beyond the empirical potentials used in the present study.

#### ACKNOWLEDGMENTS

We are grateful to R. L. McGreevy, D. A. Keen, and V. M. Nield for sending us the results of their neutron-scattering data and reverse Monte Carlo studies in advance of publication. M.S. thanks S. Tamaki, H. Okazaki, and M. Kobayashi for several useful discussions

held during a research visit to Niigata University. He also thanks the hospitality of the Department de Física i Enginyeria Nuclear of the Universitat Politècnica de Catalunya during a research visit when this work was com-

pleted. A.G. and J.T. thank Y. Ossetsky for useful discussions. Financial support by the DGICYT (Spain) through Grant No. PB90 0631 is gratefully acknowledged.

- 
- <sup>1</sup>The term "almost-ionic solids" to characterize the noble-metal and thallium halide compounds was first coined, to our knowledge, by M. P. Tosi, in *Solid State Physics: Advances in Research and Applications*, edited by F. Seitz and D. Turnbull (Academic, New York, 1964), Vol. 16, p. 1.
- <sup>2</sup>See J. C. Phillips, *Rev. Mod. Phys.* **42**, 317 (1970).
- <sup>3</sup>We have consulted the following papers: E. Rapoport and C. W. T. F. Pistorius, *Phys. Rev.* **72**, 838 (1968); V. Meisalo and M. Kalliomäki, *High. Temp. High Press.* **5**, 663 (1973).
- <sup>4</sup>There is a vast literature on the subject. A good review on the subject is J. B. Boyce and B. A. Huberman, *Phys. Rep.* **51**, 189 (1979).
- <sup>5</sup>B. E. Mellander, *Phys. Rev. B* **26**, 5886 (1982).
- <sup>6</sup>W. Andreoni and M. P. Tosi, *Solid State Ion.* **11**, 49 (1983).
- <sup>7</sup>D. A. Keen, W. Hayes, and R. L. McGreevy, *J. Phys. Condens. Matter* **2**, 2773 (1990); V. M. Niels, D. A. Keen, W. Hayes, and R. L. McGreevy, *ibid.* **4**, 6703 (1992); V. M. Niels, Ph.D. thesis, Oxford University, 1993.
- <sup>8</sup>S. B. Korner, *Sov. Phys. Usp.* **11**, 229 (1968); H. B. Radousky, M. Ross, A. C. Mitchell, and W. J. Nellis, *Phys. Rev. B* **31**, 1457 (1985).
- <sup>9</sup>M. Ross and F. J. Rogers, *J. Phys. (Paris) Colloq.* **45**, C8-229 (1984); *Phys. Rev. B* **31**, 1463 (1985); M. Ross and G. Wolf, *Phys. Rev. Lett.* **57**, 214 (1986).
- <sup>10</sup>J. Trullàs, A. Giró, J. A. Padró, and M. Silbert, *Physica A* **171**, 384 (1991).
- <sup>11</sup>M. Silbert, A. Giró, and J. Trullàs, *Phys. Rev. B* **46**, 14 886 (1992).
- <sup>12</sup>P. Vashishta and A. Rahman, *Phys. Rev. Lett.* **40**, 1337 (1978); A. Rahman and P. Vashishta, in *Physics of Superionic Conductors*, edited by J. W. Perram (Plenum, New York, 1983), p. 93.
- <sup>13</sup>A. J. Stafford, M. Silbert, J. Trullàs, and A. Giró, *J. Phys. Condens. Matter* **2**, 6631 (1990); J. Trullàs, A. Giró, and M. Silbert, *ibid.* **2**, 6643 (1990).
- <sup>14</sup>See, e.g., W. Alda and J. Moscinski, *Philos. Mag. A* **64**, 1145 (1991).
- <sup>15</sup>D. Beeman, *J. Comput. Phys.* **20**, 130 (1976).
- <sup>16</sup>See M. J. L. Sangster and M. Dixon, *Adv. Phys.* **25**, 247 (1976).
- <sup>17</sup>P. Vashishta and A. Rahman, in *Fast Ion Transport in Solids*, edited by P. Vashishta, J. N. Mundy, and G. K. Shenoy (Elsevier, New York, 1979), p. 527.
- <sup>18</sup>A. Blacha, N. E. Christensen, and M. Cardona, *Phys. Rev. B* **33**, 2413 (1986).
- <sup>19</sup>M. Parrinello and A. Rahman, *Phys. Rev. Lett.* **45**, 1196 (1980).
- <sup>20</sup>J. Tallon, *Phys. Rev. Lett.* **57**, 2427 (1986).
- <sup>21</sup>M. J. Moore, J. S. Kasper, and F. P. Bundy, *J. Solid State Chem.* **1**, 170 (1970).
- <sup>22</sup>S. Hull and D. Keen, *Europhys. Lett.* **24**, 263 (1993).